Core-Annular Flow of Liquid Membrane Emulsion

W. S. Ho and N. N. Li
Corporate Research, Exxon Research and Engineering Company, Route 22 East, Annandale, NJ 08801

A modeling and experimental study of the core-annular flow (CAF) was carried out with a viscous liquid membrane emulsion as the core and an aqueous solution as the annulus. A hydrodynamic model has been developed for stable CAF with a centered, nondeformable core surrounded by a turbulent aqueous annulus with or without a drag reducer. This model has been verified with data from flow tests with viscous emulsions in a horizontal flow loop of 3/4-in. (19-mm) tubing and a full-scale, down-hole well tubing of 2-7/8 in. (73 mm). By the use of this model along with the data, the effects of annular size on total and core flow rates and pressure drop are investigated for annuli with and without a drag reducer.

Introduction

Core-annular flow (CAF) is an effective way for the transport of a viscous material such as heavy crude or emulsion, in which the viscous material is pumped as the core phase surrounded with an immiscible, low-viscosity fluid such as water as the annular phase. The low viscosity, annular fluid is used for lowering the pressure drop in the transport of the viscous material. CAF is shown in Figure 1.

The advantage of adding water to crude oil pipelining was first suggested by Isaacs and Speed (1904) in a U.S. patent. However, the patent went essentially unnoticed for 46 years until Clark and Shapiro (1950) patented a process for pipelining viscous crude oil by injecting water and demulsifying agents into the line. Glass (1961) investigated the addition of water as the annular phase to aid pumping viscous oils and observed 30–40% water for giving the lowest pressure drop. Kiel (1968) patented a CAF process for pumping viscous materials such as heavy petroleum fractions and water-in-oil emulsions, surrounded with an annular water phase, for fracturing subterranean formations to increase oil or gas production. In 1972 Shell Oil Co. (1972a–f) widely publicized the use of CAF with a water annulus to pipeline viscous crude without heating or insulating the line. With the water flow rate at 30% (by volume) of the total flow rate, the CAF was stable as long as the flow velocity was at least 3 ft/s. They operated the 6-in. (152-mm) diameter, 24-mile (38.6-km) long line near Bakersfield, CA. Recently, CAF pipelining of Venezuelan heavy crude took place in an 8-in. (203-mm) diameter, 0.62-mile (1-km) long test loop in San Tome and a 6-in. (152-mm) diameter, 34-mile (54.7-km) long commercial pipeline located between San Diego Norte and Budare 2 (Anon, 1988; Guevara et al., 1988, 1990).

CAF for pipelining of viscous crudes has been studied extensively (Russell and Charles, 1959; Seyer and Metzner, 1969; Ooms et al., 1984; Oliemans and Ooms, 1986; Wu et al., 1986; Guevara et al., 1988; Brauner, 1991; Bai et al., 1992). Models to relate CAF flow rates to pressure drops have been developed for stable CAF with the annular phase in the laminar flow regime (Russell and Charles, 1959; Bentwich et al., 1970; Ooms et al., 1984; Oliemans and Ooms, 1986). In the stable CAF, the core and annular phases are distinct and continuous, and their flow rates are steady with fully-developed flow patterns.

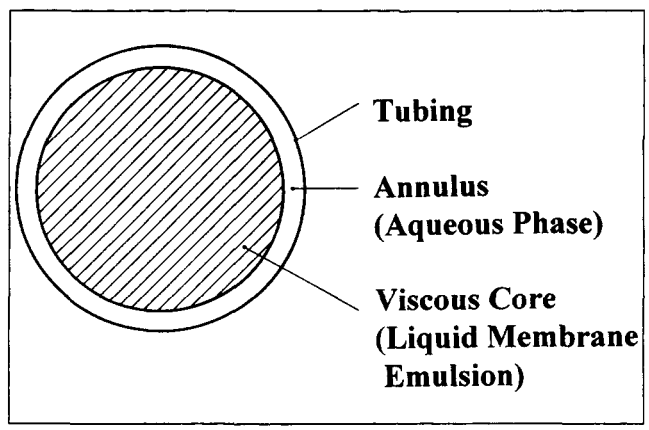

Figure 1. Core-annular flow (CAF).

Correspondence concerning this article should be addressed to W. S. Ho.
Present address of N. N. Li: Allied Signal, Inc., 50 East Algonquin Road, Des Plaines, IL 60017.

Russell and Charles (1959) solved the Navier-Stokes equation for the incompressible, laminar CAF with a concentric core to calculate pressure gradients and flow rates. Bentwich et al. (1970) used the same approach to obtain a series solution for the incompressible, laminar CAF with an eccentric core. Ooms et al. (1984) and Oliemans and Ooms (1986) developed a laminar CAF model based on the hydrodynamic lubrication theory, and they showed that the ripples on the interface moving with respect to the pipe wall can generate pressure variations in the annular layer to counterbalance the buoyancy force on the core. Oliemans et al. (1985, 1987) extended this model to incorporate the effect of turbulence in the water annulus. Recently, Arney et al. (1993) and Huang et al. (1993) investigated the friction factor and water holdup for CAF. In addition, the stability of CAF was analyzed theoretically and studied experimentally (Hasson et al., 1970; Hasson and Nir, 1970; Ooms, 1972; Garg, 1978; Preziosi et al., 1989; Hu and Joseph, 1989; Chen, 1990, 1992; Chen et al., 1990; Hu et al., 1990; Papageorgiou et al., 1990; Chen and Joseph, 1991a,b; Georgiou, 1991; Georgiou et al., 1991, 1992; Bai et al., 1992; Boomkamp and Miesen, 1992; Miesen et al., 1992).

This article reports on a modeling and experimental study of CAF for a liquid membrane emulsion surrounded with an aqueous annular phase in the turbulent flow regime. A CAF model was developed by the use of the universal velocity profiles for the annular phase. This model was used to guide the experimental work with water-in-oil emulsions prepared from diesel containing 10 vol. % polyamine surfactant and with various water-to-oil ratios up to 11. This model was compared with experimental data obtained from a horizontal flow loop of 3/4-in. (19-mm) tubing and a full-scale, down-hole well tubing of 2-7/8 in. (73 mm).

Core-Annular Flow Model

The assumptions of the core-annular flow (CAF) model for an aqueous annular phase in the turbulent flow regime are:

(1) The tubing wall is smooth;

(2) The annulus is stable, and it contains a drag reducer or it does not contain a drag reducer; the hydrodynamic equations and velocity profiles for the annulus are the same as those for one-phase flow;

(3) The core is stable and centered; it is nondeformable, that is, plug-flow, and its surface is like a rough pipe.

Based on these assumptions, this model comprises the four flow zones shown in Figure 2: the laminar sublayer of the annulus adjacent to the tubing wall, the turbulent zone of the annulus (adjacent to this laminar sublayer), the laminar sublayer of the annulus adjacent to the plug-flow core, and the plug-flow core.

The hydrodynamic equations for one-phase flow are (Schlichting, 1979; Benedict, 1980):

$$\tau = r\left(\frac{\Delta p}{2L}\right) \tag{1}$$

$$\tau = \mu \frac{du}{dy} + \rho K^2 y^2 \left(\frac{du}{dy}\right)^2 \tag{2}$$

$$u = 0 \text{ at } y = 0 \tag{3}$$

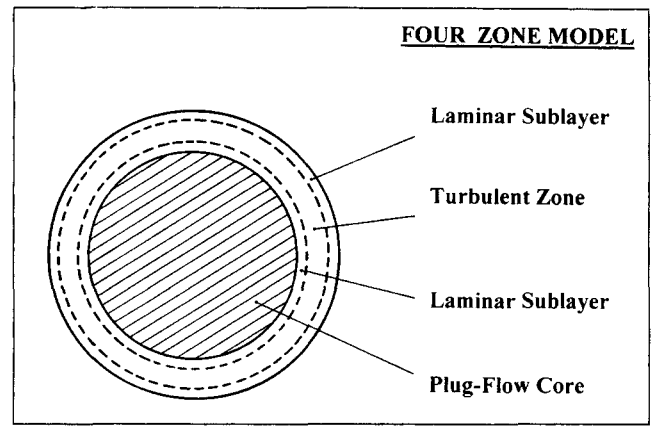

Figure 2. Four zones of the CAF model.

where τ is the shear stress, r the radial coordinate, Δp the pressure drop, L the tubing length, μ the viscosity, u the velocity, y the distance from the tubing wall, ρ the density, and K the universal constant for Prandtl's mixing length Ky. K is 0.4 for the case without a drag reducer (Schlichting, 1979; Benedict, 1980). Equation 1 derives from the momentum balance. In Eq. 2, the first term is the viscous contribution to the shear stress whereas the second term is the turbulent portion of the shear stress. Based on the second assumption described earlier, Eqs. 1-3 are used for the annulus. Through these equations, the universal velocity profiles for the laminar sublayer and turbulent zone have been obtained for one-phase flow for the two cases with and without a drag reducer (Schlichting, 1979; Benedict, 1980). Thus, the CAF model can be divided into these two cases.

Model for the annulus containing no drag reducer

The velocity profile for the laminar sublayer adjacent to the wall of a smooth tubing in dimensionless terms is:

$$u_l^+ = y^+ \quad 0 \le y^+ \le 11.6 \tag{4}$$

where

$$u^+ = \frac{u}{v^*} \tag{5}$$

$$y^+ = \frac{y v^*}{\nu} \tag{6}$$

$$v^* = \sqrt{\frac{\tau_w}{\rho}} \tag{7}$$

$$\tau_w = \frac{R\Delta p}{2L} \tag{8}$$

ν is kinematic viscosity, that is, $\nu = \mu/\rho$, τ_w the wall shear stress, and R the inside radius of the tubing (Schlichting, 1979; Benedict, 1980). As shown in Eq. 4, this velocity profile is linear. The velocity profile for the turbulent zone next to this laminar sublayer is (Schlichting, 1979; Benedict, 1980):

$$u_2^+ = 2.5 \ln y^+ + 5.5 \qquad 11.6 \le y^+ \le (y_c^+ - 5) \tag{9}$$

where y_c^+ is the dimensionless annulus width, that is, the position for the core. In this equation, y^+ equals $y_c^+ - 5$ at the position where the thickness of the laminar sublayer adjacent to the core with a surface like a rough pipe is 5 (in the dimensionless distance). The laminar sublayer thickness for a rough pipe is 5 (Schlichting, 1979). In Eqs. 4 and 9, y^+ equals 11.6 at the flow transition from the laminar sublayer to the turbulent zone where the continuity of the velocity applies, that is, $u_1^+ = u_2^+$. The velocity profile for the laminar sublayer adjacent to the core is:

$$u_3^+ = 2.5 \ln(y_c^+ - 5) + y^+ - y_c^+ + 10.5$$

$$(y_c^+ - 5) \le y^+ \le y_c^+ \tag{10}$$

This equation results from the linear velocity profile for this sublayer via the boundary condition:

$$u_3^+ = u_2^+ \quad \text{at} \quad y^+ = y_c^+ - 5 \tag{11}$$

Resulting from the following boundary condition:

$$u_4^+ = u_3^+ \quad \text{at} \quad y^+ = y_c^+ \tag{12}$$

the velocity for the plug-flow core is:

$$u_4^+ = 2.5 \ln(y_c^+ - 5) + 10.5$$

$$y_c^+ \le y^+ \le R^+ \tag{13}$$

Based on the velocity profiles, the flow rate and pressure drop relationships for the annulus and core are obtained. Integration of the velocity profiles u_1^+, u_2^+, and u_3^+, that is, Eqs. 4, 9 and 10, with respect to y^+ gives the volumetric flow rate for the annulus, Q_a:

$$Q_a = 2\pi \frac{\nu^2}{v^*} [(2.5\, R^+ y_c^+ - 1.25\, y_c^{+2}) \ln(y_c^+ - 5) + 3\, R^+ y_c^+ - 2.125\, y_c^{+2} - 13.6\, R^+ - 18.75\, y_c^+ + 214.4] \tag{14}$$

Dropping out the two small terms 18.75 y_c^+ and 214.4 in Eq. 14 results in:

$$Q_a = 2\pi \frac{\nu^2}{v^*} [(2.5\, R^+ y_c^+ - 1.25\, y_c^{+2}) \ln(y_c^+ - 5) + 3\, R^+ y_c^+ - 2.125\, y_c^{+2} - 13.6\, R^+] \tag{15}$$

Similarly, integration of u_4^+, that is, Eq. 13, with respect to y^+ gives the volumetric flow rate for the core, Q_c:

$$Q_c = \pi \frac{\nu^2}{v^*} (R^+ - y_c^+)^2 [2.5 (\ln y_c^+ - 5) + 10.5] \tag{16}$$

the total flow rate Q_t is:

$$Q_t = Q_a + Q_c \tag{17}$$

Model for the annulus containing a drag reducer

For this model, the velocity profile for the laminar sublayer adjacent to the wall of a smooth tubing in dimensionless terms is the same as that for the model with the annulus containing no drag reducer, that is, Eq. 4. This is based on the fact that in laminar flow, drag reducers do not change practically the pressure drop and the laminar sublayer thickness (Schlichting, 1979). As mentioned before, the sublayer velocity profile is linear. Also, Eqs. 5-8 apply for the model with the annulus containing a drag reducer. The velocity profile for the turbulent zone, which is next to this laminar sublayer and in which the drag reducer exhibits the ultimate velocity profile, is (Virk, 1971; Schlichting, 1979):

$$u_2^+ = 11.7 \ln y^+ - 17 \qquad 11.6 \le y^+ \le (y_c^+ - 5) \tag{18}$$

The boundaries of this turbulent zone, that is, $11.6 \le y^+ \le (y_c^+ - 5)$, are the same as those for the model with the annulus containing no drag reducer described earlier. The velocity profile for the laminar sublayer adjacent to the core is:

$$u_3^+ = 11.7 \ln(y_c^+ - 5) + y^+ - y_c^+ - 12$$

$$(y_c^+ - 5) \le y^+ \le y_c^+ \tag{19}$$

In the same way as Eq. 10, Eq. 19 results from the linear velocity profile for this sublayer via the boundary condition, Eq. 11. Similarly, resulting from the boundary condition, Eq. 12, the velocity profile for the plug-flow core is:

$$u_4^+ = 11.7 \ln(y_c^+ - 5) - 12$$

$$y_c^+ \le y^+ \le R^+ \tag{20}$$

In the similar way described earlier, integration of the velocity profiles u_1^+, u_2^+, and u_3^+, that is, Eqs. 4, 18 and 19, with respect to y^+ leads to the volumetric flow rate for the annulus, Q_a:

$$Q_a = 2\pi \frac{\nu^2}{v^*} [(11.7\, R^+ y_c^+ - 5.85\, y_c^{+2}) \ln(y_c^+ - 5) - 28.7\, R^+ y_c^+ + 11.45\, y_c^{+2} + 138.6\, R^+] \tag{21}$$

Similarly, integration of u_4^+, that is, Eq. 20, with respect to y^+ results in the volumetric flow rate for the core, Q_c:

$$Q_c = \pi \frac{\nu^2}{v^*} (R^+ - y_c^+)^2 [11.7 \ln(y_c^+ - 5) - 12] \tag{22}$$

The total flow rate Q_t is Eq. 17.

Experimental

The core-annular flow (CAF) of a liquid membrane emulsion surrounded with an aqueous annular phase in the turbulent

flow regime was conducted experimentally. The emulsions used were of the water-in-oil type. In the emulsions, the oil phase was a solution of 10 vol. % ECA 5025 polyamine surfactant in diesel, whereas the internal water phase was an aqueous solution of 2 wt. % KCl. The water/oil volume ratios were from 5 up to 11. The emulsions were prepared by pumping the aqueous solution gradually into a ribbon blender containing the oil phase while this blender was operated at a rotation speed of 60 rpm. This preparation resulted in the emulsions containing coarse droplets with a viscosity of about 14,000 cp (140 poise) at 1 s^{-1} shear rate (measured via a Fann viscometer). The relatively low viscosity emulsions were stiffened via a centrifugal pump. The viscous emulsions had a viscosity greater than 120,000 cp at 1 s^{-1}. The densities at 23°C were 0.846 g/cm^3 for the oil phase and 1.012 g/cm^3 for the aqueous phase. The density of the emulsion used mostly with a water/oil volume ratio of 11 was 0.998 g/cm^3 at the same temperature.

The aqueous annular phases used were 2 wt. % KCl solutions with and without the 240 ppm drag reducer of FR-20, which was a copolymer of acrylamide and 2-acrylamido-2-methylpropanesulfonic acid with a molecular weight of about 6 million. The annular phase without the drag reducer had a viscosity of 1.1 cp and a density of 1.012 g/cm^3 at 23°C, whereas the annular phase with the drag reducer had 1.4 cp and 1.012 g/cm^3 at the same temperature. For comparison, the water with this drag reducer used for one-phase flow had a viscosity of 1.25 cp and a density of 1 g/cm^3 at the same temperature.

Flow rate and pressure drop data were obtained via magnetic flowmeters and pressure transducers from a 306-ft horizontal flow loop of 3/4-in. (19-mm) tubing and a 10,000-ft full-scale, down-hole well tubing of 2-7/8 in. (73 mm). The 3/4-in. (19-mm) tubing had an inside radius of 0.787 cm (0.31 in.), and the 2-7/8-in. tubing had an inside radius of 3.10 cm (1.22 in.).

Results and Discussion

CAF with the annulus containing no drag reducer

The effect of annular size expressed in terms of the ratio of the annulus width y_c to the tubing radius R on pressure drop for a total flow rate of 16.3 gal/min (61.7 L/min or 1,028 cm^3/s) in the 3/4-in. tubing is shown in Figure 3. In this figure, the pressure drop relative to water is the ratio of the pressure drop for the CAF to that for the one-phase flow of water (the pressure drop for the one-phase water flow at 16.3 gal/min was 74 psi/100 ft [16.7 kPa/m or 1,670 dyne/cm^3]. The solid curve in this figure is the modeling result calculated from Eqs. 15-17. As shown in this figure, the pressure drop for a given total flow rate reduces sharply first, then reaches a minimum, and finally increases gradually to approach the pressure drop of the one-phase flow of water as the ratio of the annulus width to the tubing radius increases. Thus, annular size affects the pressure drop of CAF significantly, and the model shows an optimal annular size for the minimum pressure drop. Also shown in this figure is a datum for the CAF with an annular flow rate/total flow rate ratio (Q_a/Q_t) of 0.14 corresponding to an annulus width/tubing radius ratio (y_c/R) of 0.1 (Q_a/Q_t was controllable experimentally through the pumping rates, and it was related to y_c/R via the model) and a viscous liquid membrane emulsion with a viscosity of about 140,000 cp (1,400 poise) at 1 s^{-1}. This datum corresponds to a pressure drop of

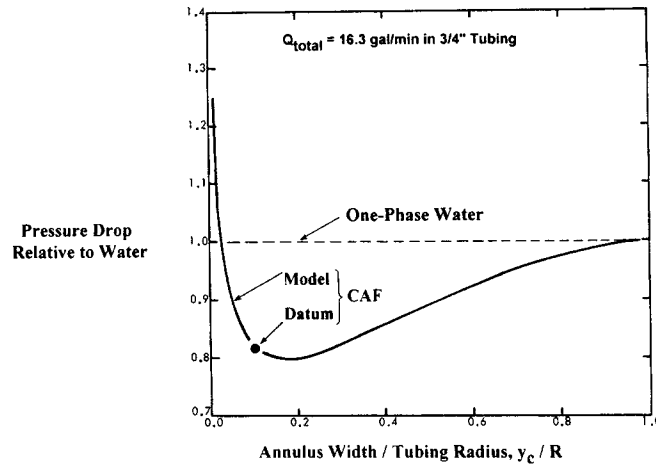

Figure 3. Annular size affects pressure drop significantly.

The model shows the optimal annular size for the minimum pressure drop at a given total flow rate for the annulus containing no drag reducer.

60 psi/100 ft (13.57 kPa/m or 1,357 dyne/cm^3) for the total CAF rate of 16.3 gal/min ($Q_a = 2.28$ gal/min and $Q_c = 14.0$ gal/min). As shown in this figure, this datum agrees quite well with the modeling result.

Figure 4 shows the effect of annular size on the total and core flow rates of the CAF for a pressure drop of 60 psi/100 ft (13.57 kPa/m or 1,357 dyne/cm^3) in the 3/4-in. (19-mm) tubing. In this figure, the flow rates relative to water are the ratios of the CAF rates to the flow rate of the one-phase flow of water (the one-phase water flow rate was 14.5 gal/min (54.9 L/min or 915 cm^3/s) for the pressure drop of 60 psi/100 ft). The total and core flow rates shown in solid lines in this figure were calculated from Eqs. 15-17. As shown in this figure, the flow rates increase sharply first, then reach their maxima, and finally reduce gradually with increasing annular size. Thus, annular size influences the flow rates significantly. The model gives the optimal annular sizes or Q_a/Q_t ratios for the maximum total and core flow rates. The optimal annular sizes for

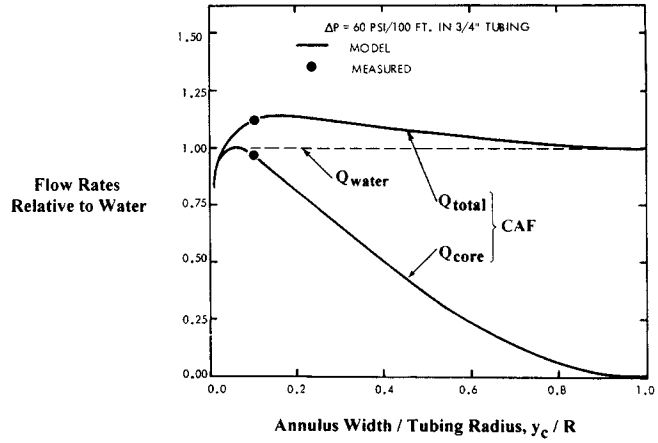

Figure 4. Flow rates change with annular size.

The model gives the optimal annular size for the maximum core or total flow rate at a given pressure drop for the annulus containing no drag reducer.

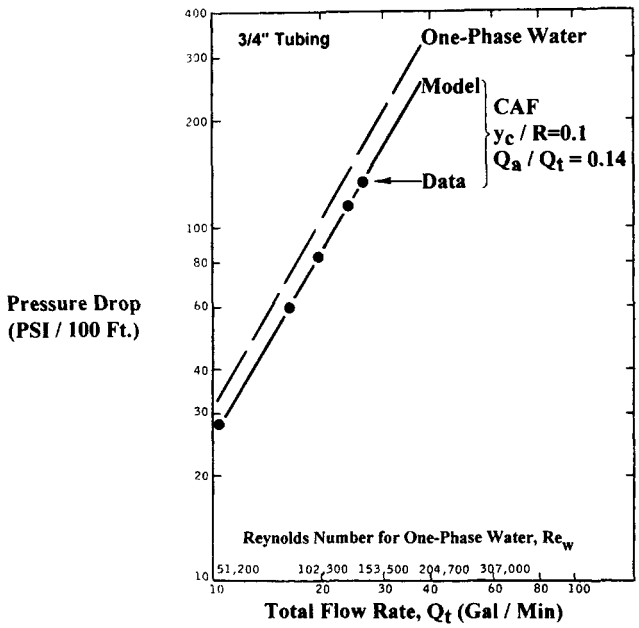

Figure 5. Core-annular flow can reduce pressure drop for the annulus containing no drag reducer.

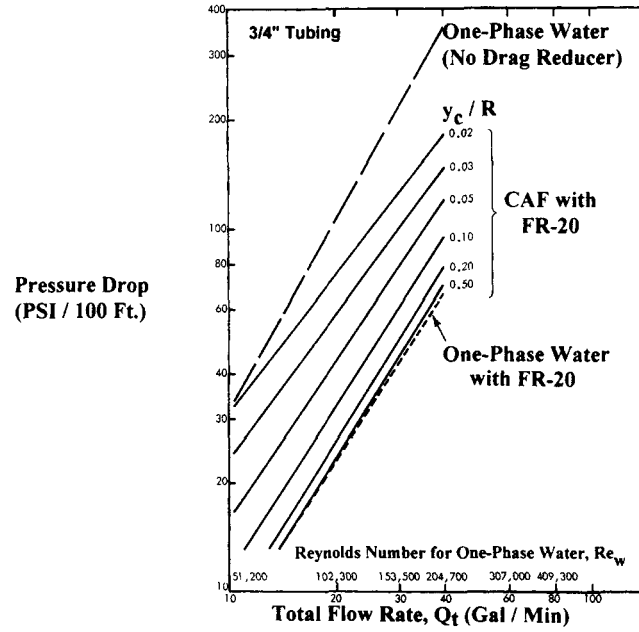

Figure 7. Predicted pressure drop vs. total flow rate and Reynolds number for various annular sizes for the annulus containing a drag reducer.

the maximum flow rates are close to an annulus width/tubing radius ratio of 0.1 corresponding to a Q_a/Q_t ratio of 0.14. For this annular size, the flow rates measured were $Q_t = 16.3$ gal/min and $Q_c = 14.0$ gal/min, and they are also shown in this figure for comparison with the modeling results. These measured flow rates agree very well with the modeling results.

At the annular flow rate/total flow rate ratio of 0.14, that is, at the annulus width/tubing radius ratio of 0.1 (close to the optimal annular size), pressure drops were measured at various total flow rates in the 3/4-in. (19-mm) tubing. Figure 5 shows the measured results in good agreement with those calculated from the model. Also shown in Figure 5 is the flow rate and pressure drop relationship for the one-phase flow of water. As shown in this figure, the pressure drop for the CAF at a given total flow rate is lower than that for the one-phase water flow. In other words, the CAF can reduce pressure drop. Also shown in this figure, the Reynolds numbers for the one-phase water flow, Re_w, are greater than 51,200, that is, the flow regime is turbulent.

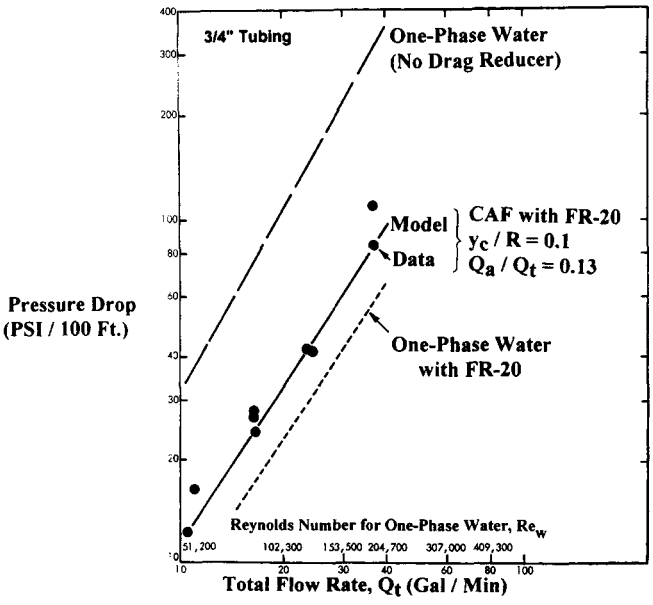

Figure 6. Drag reducer further reduces pressure drop.

CAF with the annulus containing a drag reducer

Flow rate and pressure drop data for the CAF with the annulus containing 240 ppm FR-20 drag reducer in the 3/4-in. (19-mm) tubing were obtained for an annular flow rate/total flow rate ratio (Q_a/Q_t) of 0.13 corresponding to an annulus width/tubing radius ratio of 0.1 (which is close to the optimal annular size for the annulus without a drag reducer). Figure 6 shows the data in good agreement with the modeling results calculated from Eqs. 21, 22, and 17. Also shown in Figure 6 are the flow rate and pressure drop relationships for the one-phase flows of water with and without 240 ppm FR-20 drag reducer. As shown in this figure, the pressure drop for the CAF with this drag reducer at a given total flow rate is much lower than that for the one-phase of water without this drag reducer. As seen from comparing this figure with Figure 5, the pressure drop for the CAF with this drag reducer is also lower than that for the CAF without this drag reducer. Thus, the drag reducer further reduces pressure drop.

As shown in Figure 6, the pressure drop for the CAF with 240 ppm FR-20 drag reducer for a given total flow rate is higher than that for the one-phase flow of water with the same drag reducer at the same concentration. Figure 7 shows the predicted relationship between pressure drop and total flow rate/Reynolds number at various annular sizes in terms of the annulus width/tubing radius ratio, y_c/R, for the CAF with

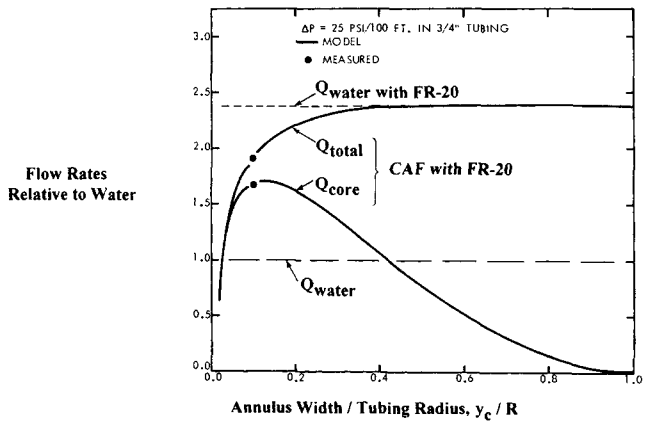

Figure 8. Flow rates change with annular size.

The model gives the optimal annular size for the maximum core flow rate at a given pressure drop for the annulus containing a drag reducer.

this drag reducer in the 3/4-in. tubing. As shown in this figure, at the annular size, $y_c/R = 0.5$, the pressure drop for the CAF approaches that for the one-phase flow of water with this drag reducer.

Figure 8 shows the modeling results for the effects of annular size on the total and core flow rates of the CAF with the drag reducer at a given pressure drop of 25 psi/100 ft (5.65 kPa/m or 565 dyne/cm^3) in the 3/4-in. (19-mm) tubing. As the annular size increases, the total flow rate increases sharply first and then approaches the flow rate of the one-phase flow of the water with this drag reducer. The core flow rate increases sharply first, then reaches a maximum, and finally reduces as the annulus width/tubing radius ratio increases. Thus, the model gives the optimal annular size for the maximum core flow rate. The optimal annulus width/tubing radius ratio is about 0.11. As shown in this figure, at the annular flow rate/total flow rate ratio of 0.13 corresponding to the annulus width/tubing radius ratio of 0.1, which is close to the optimal annular size for the maximum core flow rate, the measured

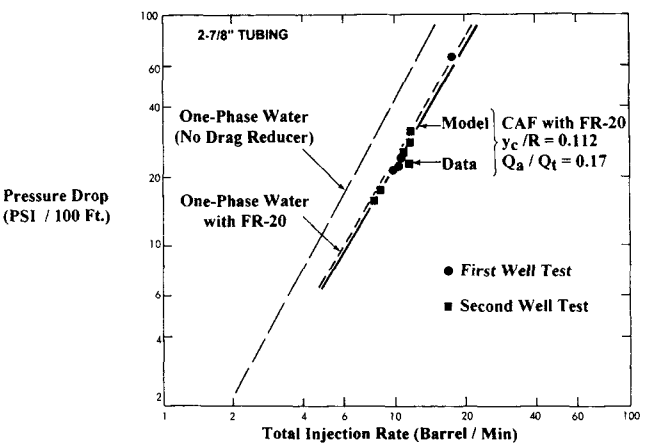

Figure 9. The model agrees with data for injection in a full-scale, down-hole well tubing of 2-7/8 in. (73 mm) for the annulus containing a drag reducer.

results for the total and core flow rates agree well with the modeling results. Also shown in this figure, the total and core flow rates for the annular size close to the optimal value for the maximum core flow rate are much larger than the flow rate of the one phase of water without this drag reducer.

With an annular flow rate/total flow rate ratio of 0.17 corresponding to an annulus width/tubing radius ratio of 0.112, which is about the optimal annular size for the maximum core flow rate, two CAF tests were conducted in a 10,000-ft (3-km) full-scale, down-hole well tubing of 2-7/8 in. (73 mm). In these tests, the annulus contained the same drag reducer at the same concentration. Figure 9 shows the total injection rate and pressure drop results from these tests. As shown in this figure, the results from the second well test agree quite well with those from the first test. All these results are in good agreement with those calculated from the model. The density of the emulsion used with a water/oil volume ratio of 11 (0.998 g/cm^3 at 23°C) was quite close to that of the annular phase (1.012 g/cm^3 at 23°C). The effect of the density difference was neglected in the model.

Also shown in Figure 9 for comparison are the flow rate and pressure drop relationships for the one-phase water flows with and without this drag reducer. The pressure drop for the CAF at a given total flow rate is lower than that for the one-phase water flow with the same drag reducer. Thus, the CAF can reduce pressure drop. Certainly, the pressure drop for the CAF is much lower than that for the one-phase water flow without a drag reducer.

A comparison between Figures 6 and 9 shows the effect of tubing size on the pressure drop-flow rate relationship. As described earlier, for the smaller tubing size of 3/4 in. in Figure 6, the pressure drop for the CAF at a given total flow rate is higher than that for the one-phase water flow with the same drag reducer, whereas for the larger tubing size of 2-7/8 in. in Figure 9, the reverse is the case. From Eqs. 18, 6 and 8, the velocity in the turbulent zone increases as y^+, that is, y or y_c increases. Thus, a larger tubing gives a larger velocity in the turbulent zone for a given y_c/R ratio (about 0.1 for the cases considered). The pressure drop for a given total flow rate reduces as y_c, that is, y_c/R for a given tubing increases as shown in Figure 7. Therefore, the tubing size affects the pressure drop/flow rate behavior.

All emulsions used for all CAF results discussed above were viscous with a viscosity of greater than 120,000 cp (1,200 poise) at 1 s^{-1}, and they had water/oil volume ratios ranging from 7 to 11. These viscous emulsions gave stable CAF, allowing flow rate and pressure drop results to be predictable via the model.

The effect of the viscosity of emulsion core on pressure drop for the CAF with the annulus containing the drag reducer in the 3/4-in. tubing was examined by the use of the emulsions with viscosities ranging from about 65,000 to 113,000 cp (650 to 1,130 poise) at 1 s^{-1}. The emulsions had a water/oil volume ratio of 5. The ratio of the annular and total flow rates, Q_a/Q_t, was 0.13, that is, the annulus width/tubing radius ratio, y_c/R, was 0.1, which was about the optimal annular size. The total flow rates ranged from 11 to 25 gal/min (41.6 to 94.6 L/min or 693 to 1,577 cm^3/s). Figure 10 shows the effect of emulsion viscosity on pressure drop. For a viscosity of less than 110,000 cp, the pressure drop increased as emulsion viscosity reduced. When the emulsion viscosity was lower than

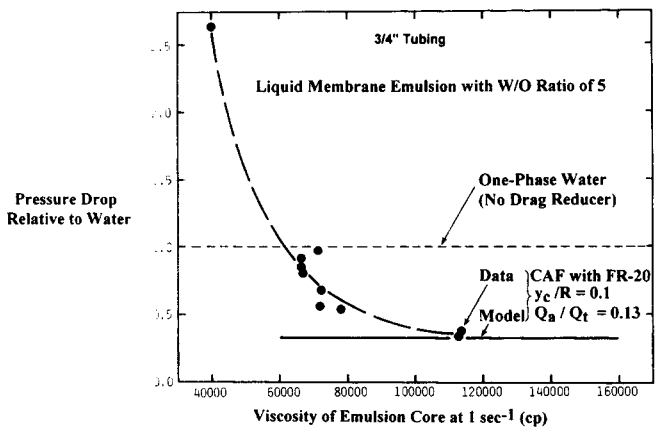

Figure 10. Pressure drop increased as emulsion viscosity reduced for a viscosity of less than 110,000 cp (for the annulus containing a drag reducer).

about 60,000 cp (at 1 s^{-1}), the pressure drop was greater than that for the one-phase water flow without a drag reducer. This was presumably due to the deformation of the emulsion core by the annulus and/or the dispersion of the emulsion in the annulus. Nevertheless, the pressure drop approached that predicted via the model when the emulsion viscosity was greater than about 110,000 cp (at 1 s^{-1}).

Conclusions

Core-annular flow (CAF) can reduce pressure drop significantly. The pressure drop for CAF at a given flow rate can be lower than that for the one-phase flow of a liquid used as the annulus of the CAF. A hydrodynamic model has been developed for stable CAF with a centered, nondeformable core surrounded by a turbulent aqueous annulus with or without a drag reducer. This model can predict the flow rate and pressure drop results for the CAF of a viscous liquid membrane emulsion with a viscosity of greater than 120,000 cp at 1 s^{-1}. This model can also predict the optimal annular size for the minimum pressure drop at a given total or core flow rate or for the maximum core flow rate at a given pressure drop. In addition, this model shows significant effects of annular size on flow rates and pressure drop.

Notation

K = universal constant for Prandtl's mixing length
L = tubing length, cm
p = pressure, dyne/cm^2
Δp = pressure drop, dyne/cm^2
Q_a = annular flow rate, cm^3/s
Q_c = core flow rate, cm^3/s
Q_t = total flow rate, cm^3/s
r = radial coordinate, cm
R = inside radius of the tubing, cm
R^+ = dimensionless tubing radius
u = velocity, cm/s
u^+ = dimensionless velocity
u_1^+ = dimensionless velocity for the laminar sublayer adjacent to the tubing wall
u_2^+ = dimensionless velocity for the turbulent zone
u_3^+ = dimensionless velocity for the laminar sublayer adjacent to the core
u_4^+ = dimensionless velocity for the plug-flow core
v^* = friction velocity defined in Eq. 7, cm/s
y = distance from the tubing wall, cm
y^+ = dimensionless distance from the tubing wall
y_c = distance between the tubing wall and core (annulus width), cm
y_c^+ = dimensionless annulus width

Greek letters

μ = viscosity, poise or dyne·s/cm^2
ν = kinematic viscosity ($\nu = \mu/\rho$), poise·cm^3/g or dyne·cm·s/g
ρ = density, g/cm^3
τ = shear stress, dyne/cm^2
τ_w = wall shear stress, dyne/cm^2

Literature Cited

Anon, "Venezuelan Line to Carry Heavy Oil in Water Film," *Oil Gas J.*, **86**, 112 (1988).

Arney, M. S., R. Bai, E. Guevara, D. D. Joseph, and K. Liu, "Friction Factor and Holdup Studies for Lubricated Pipelining: I. Experiments and Correlations," *Int. J. Multiphase Flow*, **19**, 1061 (1993).

Bai, R., K. Chen, and D. D. Joseph, "Lubricated Pipelining: Stability of Core-Annular Flow: 5. Experiments and Comparison with Theory," *J. Fluid Mech.*, **240**, 97 (1992).

Benedict, R. P., *Fundamentals of Pipe Flow*, Chap. 5, Wiley, New York (1980).

Bentwich, M., D. A. I. Kelly, and N. Epstein, "Two-Phase Eccentric Interface Laminar Pipeline Flow," *J. Basic Eng. Trans. ASME Ser. D*, **92**, 32 (1970).

Boomkamp, P. A. M., and R. H. M. Miesen, "Nonaxisymmetric Waves in Core-Annular Flow with a Small Viscosity Ratio," *Phys. Fluids A*, **4**, 1627 (1992).

Brauner, N., "Two-Phase Liquid-Liquid Annular Flow," *Int. J. Multiphase Flow*, **17**, 59 (1991).

Chen, K., R. Bai, and D. D. Joseph, "Lubricated Pipelining: 3. Stability of Core-Annular Flow in Vertical Pipes," *J. Fluid Mech.*, **214**, 251 (1990).

Chen, K., "Short Wave Instability of Core-Annular Flow," *Phys. Fluids A*, **4**, 186 (1992).

Chen, K., "Lubricated Pipelining: The Stability of Core-Annular Flow (CAF)," PhD Diss., Univ. of Minnesota (1990).

Chen, K., and D. D. Joseph, "Lubricated Pipelining: Stability of Core-Annular Flow: 4. Ginzburg-Landau Equations," *J. Fluid Mech.*, **227**, 587 (1991a).

Chen, K., and D. D. Joseph, "Long Wave and Lubrication Theories for Core-Annular Flow," *Phys. Fluids A*, **3**, 2672 (1991b).

Clark, A. F., and A. Shapiro, "Method of Pumping Viscous Petroleum," U. S. Patent 2,533,878 (1950).

Garg, V. K., "On the Stability of Axial Flow in an Annulus," *J. Phys. Soc. Japan*, **45**, 652 (1978).

Georgiou, E., "Linear Interfacial Stability of a Core-Annular Flow With Application to Liquid-Liquid Displacements in Small Pores," PhD Diss., City Univ. of New York (1991).

Georgiou, E., C. Maldarelli, D. T. Papageorgiou, and D. S. Rumschitzki, "An Asymptotic Theory for the Linear Stability of a Core-Annular Flow in the Thin Annular Limit," *J. Fluid Mech.*, **243**, 653 (1992).

Georgiou, E., D. T. Papageorgiou, C. Maldarelli, and D. S. Rumschitzki, "The Double Layer-Capillary Stability of an Annular Electrolyte Film Surrounding a Dielectric-Fluid Core in a Tube," *J. Fluid Mech.*, **226**, 149 (1991).

Glass, W., "Water Addition Aids Pumping Viscous Oils," *Chem. Eng. Prog.*, **57**, 116 (1961).

Guevara, E., K. Zagustin, J. Paterno, J. L. Trallero, V. Zubillaga, G. Zamora, and T. Diaz, "Research and Development in Core-Annular Flow," *Rev. Tec. INTEVEP*, **10**, 63 (1990).

Guevara, E., K. Zagustin, V. Zubillaga, and J. L. Trallero, "Core-Annular Flow (CAF): The Most Economical Method for the Transportation of Viscous Hydrocarbons," 4th UNITAR/U.N. Dev. Program AOSTRA-Petro-Can.-Pet. Venez. S.A.-DOE "Heavy Crude Tar Sands," Int. Conf. Edmonton, Vol. 5, Prepr. No. 194 (Aug. 7-12, 1988).

Hasson, D., U. Mann, and A. Nir, "Annular Flow of Two Immiscible Liquids: I. Mechanism," *Can. J. Chem. Eng.*, **48**, 514 (1970).
Hasson, D., and A. Nir, "Annular Flow of Two Immiscible Liquids: II. Analysis of Core-Liquid Ascent," *Can. J. Chem. Eng.*, **48**, 521 (1970).
Hu, H. H., and D. D. Joseph, "Lubricated Pipelining: Stability of Core-Annular Flow," *J. Fluid Mech.*, **205**, 359 (1989).
Hu, H. H., T. S. Lundgren, and D. D. Joseph, "Stability of Core-Annular Flow with a Small Viscosity Ratio," *Phys. Fluids A*, **2**, 1945 (1990).
Huang, A., C. Christodoulou, and D. D. Joseph, "Friction Factor and Holdup Studies for Lubricated Pipelining: II. Laminar and k-E Models of Eccentric Core Flows," *AHPCRC Preprint* 93-064, Univ. of Minnesota (1993).
Isaacs, J. D., and J. B. Speed, "Method of Piping Fluids," U. S. Patent 759,374 (1904).
Keil, O. M., "Method for Fracturing Subterranean Formations," U.S. Patent 3,378,047 (1968).
Miesen, R., G. Beijnon, P. E. M. Duijvestijn, R. V. A. Oliemans, and T. Verheggen, "Interfacial Waves in Core-Annular Flow," *J. Fluid Mech.*, **238**, 97 (1992).
Oliemans, R. V. A., and G. Ooms, "Core-Annular Flow of Oil and Water through a Pipeline," *Multiphase Sci. Technol.*, **2**, 427 (1986).
Oliemans, R. V. A., G. Ooms, H. L. Wu, and A. Duijvestijn, "Core-Annular Oil/Water Flow: The Turbulent-Lubricating-Film Model and Measurements in a 2 in. Pipe Loop," *Soc. Pet. Eng. Middle East Oil Conf. Proc.*, No. 13725, Manama Bahrain, p. 365 (Mar. 11-14, 1985).
Oliemans, R. V. A., G. Ooms, H. L. Wu, and A. Duijvestijn, "Core-Annular Oil/Water Flow: The Turbulent-Lubricating-Film Model and Measurements in a 5 cm Pipe Loop," *Int. J. Multiphase Flow*, **13**, 23 (1987).
Oooms, G., "The Hydrodynamic Stability of Core-Annular Flow of Two-Ideal Liquids," *Appl. Sci. Res.*, **26**, 147 (1972).
Ooms, G., A. Segal, and A. J. van der Wees, "A Theoretical Model for Core-Annular Flow of a Very Viscous Oil Core and a Water Annulus through a Horizontal Pipe," *Int. J. Multiphase Flow*, **10**, 41 (1984).
Papageorgiou, D. T., C. Maldarelli, and D. S. Rumschitzki, "Nonlinear Interfacial Stability of Core-Annular Film Flows," *Phys. Fluids A*, **2**, 340 (1990).
Preziosi, L., K. Chen, and D. D. Joseph, "Lubricated Pipelining: Stability of Core-Annular Flow," *J. Fluid Mech.*, **201**, 323 (1989).
Russell, T. W. F., and M. E. Charles, "The Effect of the Less Viscous Liquid in the Laminar Flow of Two Immiscible Liquid," *Can. J. Chem. Eng.*, **37**, 13 (1959).
Schlichting, H., *Boundary Layer Theory*, 7th ed., Chap. XX, McGraw-Hill, New York (1979).
Seyer, F. A., and A. B. Metzner, "Drag Reduction in Large Tubes and the Behavior of Annular Films of Drag Reducing Fluids," *Can. J. Chem. Eng.*, **47**, 525 (1969).
Shell Oil Co., "Water Aids Flow in Pipeline," *Chem. Eng. News*, **50**, 15 (1972a).
Shell Oil Co., "Oil-Water Line Moves Highly Viscous Crude," *Oil Gas J.*, **70**, 37 (1972b).
Shell Oil Co., "New Concept Reduces Cost to Transport Heavy Crude," *Pipe Line Ind.*, **36**, 38 (1972c).
Shell Oil Co., "A Flowing Jacket of Water Enables Viscous Oil to be Carried through Bare Pipelines," *Chem. Eng.*, **79**, 53 (1972d).
Shell Oil Co., "How Shell Moves Viscous Oil in Water," *Pet. Petrochem. Int.*, **12**, 100 (1972e).
Shell Oil Co., "Shell Moves Viscous Oil through Unheated Lines," *Pipe Line News*, **44**, 26 (1972f).
Virk, P. S., "An Elastic Sublayer Model for Drag Reduction by Dilute Solution of Linear Macromolecules," *J. Fluid Mech.*, **45**, 417 (1971).
Wu, H. L., P. E. M. Duijvestijn, J. Paterno, and E. Guevara, "Core-Annular Flow: A Solution to Pipeline Transportation of Heavy Crude Oils," *Rev. Tec. INTEVEP*, **6**, 17 (1986).

Manuscript received July 23, 1993, and revision received Dec. 20, 1993.